Reactive Intermediates

DOI: 10.1002/anie.201203602

Characterization of a Thiolato Iron(III) Peroxy Dianion Complex**

Aidan R. McDonald, Katherine M. Van Heuvelen, Yisong Guo, Feifei Li, Emile L. Bominaar, Eckard Münck, and Lawrence Que Jr.**

Thiolate ligation to iron plays a vital role in the enzymatic deactivation of reactive oxygen species. Superoxide reductase (SOR) found in microaerophiles catalyzes the reduction of superoxide ($O_2^{\bullet-}$), yielding H_2O_2[1] and has an active site that consists of an iron center with four equatorial His ligands and an axial Cys ligand. The thiolate is proposed to stabilize the O–O bond of RS-$Fe^{III}(\eta^1\text{-}OO(^-/H))$ intermediates and to weaken the Fe–(OO) bond to facilitate formation of H_2O_2.[1,2] Evidence for an intermediate in the reaction between $O_2^{\bullet-}$ and SOR has been obtained, which exhibits a visible absorption feature at about 600 nm.[3] Pulse radiolysis studies showed diffusion-controlled pH-independent formation of the intermediate, while its decay was found to be pH-dependent. These results led to the postulation of the intermediate as an RS-$Fe^{II}(OO^{\bullet})$ adduct or the isoelectronic RS-$Fe^{III}(OO^-)$; however its short lifetime has made it difficult to establish the iron oxidation state experimentally. We have thus endeavored to obtain a synthetic analogue of this intermediate.

A number of synthetic non-heme RS-$Fe^{III}(\eta^1\text{-}OOX)$ (X = H, alkyl) complexes have been reported recently,[4] providing insights into the role thiolate ligation plays in modulating the reactivity of peroxide complexes, and the nature of the RS-$Fe^{III}(\eta^1\text{-}OOH)$ intermediate observed in SOR (Table 1). However, there are no reports detailing the isolation of an RS-$Fe^{III}(\eta^1\text{-}OO^-)$ complex. Herein, we describe the spectroscopic characterization of a synthetic complex that serves to model the putative RS-$Fe^{III}(\eta^1\text{-}OO^-)$ intermediate found in SOR.

Table 1: Properties of SOR and related RS-Fe^{III}(OOX) complexes.

	λ_{max} [nm] (ε, [L mol^{-1} cm^{-1}])	*r* (Fe–S) [Å]	*r* (Fe–OO) [Å]
wt-SOR_{ox} [RS-Fe^{III}(Glu)][3c,9a]	644 (1900)	2.42–2.46	
wt-SOR_{red} + superoxide[3]	600 (2800)		
E114 A-SOR_{ox} + H_2O_2 [RS-Fe^{III}(OOH)][3b,9b]	560	2.5	2.0
chloroperoxidase Cpd 0[10]		2.4	1.9
2 [Fe^{III}(TMCS)(η^1-OO^-)]	460 (6100), 610 (1200)	2.41	1.89
$[Fe^{III}(cyclam\text{-}PrS)(OOH)]^{+}$[4c]	535 (1350)		
$[Fe^{III}(S^{Me2}N_4tren)(OOH)]^{+}$[4a,h]	452 (2780)	2.33	1.86
$[Fe^{III}([15]aneN_4)(SAr)(OOR)]^{+}$[4b,d]	ca. 525	2.29–2.32	1.82–1.85
$[Fe^{III}(Me_4[15]aneN_4)(SPh)(OOR)]^{+}$[4f,g]	340 (3500), 405 (2300), 650 (2300)		

[Fe^{II}(TMCS)]PF_6 (**1**) acts as an ideal mimic of the SOR active site because it contains four equatorial N ligands and an axial S bound to the iron center (Scheme 1).[5] Compound

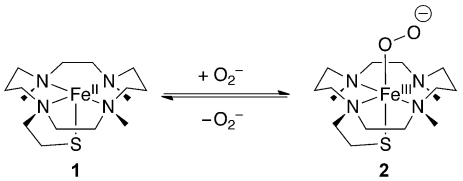

Scheme 1. Equilibrium between **1** and **2**.

1 reacted with KO_2 (dissolved in pure DMF in the presence of 2 equiv of [18]crown-6) at −90 °C in a 4:1 THF/DMF solvent mixture. The characteristic UV feature of **1** (λ_{max} = 320 nm, Figure 1) disappeared over the course of 10 s and was replaced by two new intense features (λ_{max} = 460, 610 nm), which were assigned to transient species **2**. The visible features achieved maximum intensity when an excess (> 50-fold) of KO_2 was used. Intermediate **2** was reasonably stable at −90 °C, decaying over the course of about 3 h to produce **1** nearly quantitatively (Supporting Information, Figure S1). Species **2** could then be regenerated by replenishing the KO_2. These observations suggest that superoxide binding to **1** is reversible, with the decay of **2** presumably reflecting the loss of KO_2 owing to its gradual disproportionation in the reaction

[*] Dr. A. R. McDonald, Dr. K. M. Van Heuvelen, Dr. F. Li, Prof. Dr. L. Que Jr.
Department of Chemistry, University of Minnesota
207 Pleasant Street SE, Minneapolis, MN 55455 (USA)
E-mail: larryque@umn.edu
Dr. Y. Guo, Prof. Dr. E. L. Bominaar, Prof. Dr. E. Münck
Department of Chemistry, Carnegie Mellon University
4400 Fifth Avenue, Pittsburgh, PA 15213 (USA)
E-mail: emunck@cmu.edu

[**] This work was supported by the US National Science Foundation (grant CHE1058248 to L.Q.) and the US National Institutes of Health (grant EB001475 to E.M. and postdoctoral fellowships to A.R.McD. (GM087895) and K.M.V.H. (GM093479). XAS data were collected at beamline X3B of the National Synchrotron Light Source at the Brookhaven National Laboratory, which is supported by the U.S. NIH and DOE.

Supporting information for this article is available on the WWW under http://dx.doi.org/10.1002/anie.201203602.

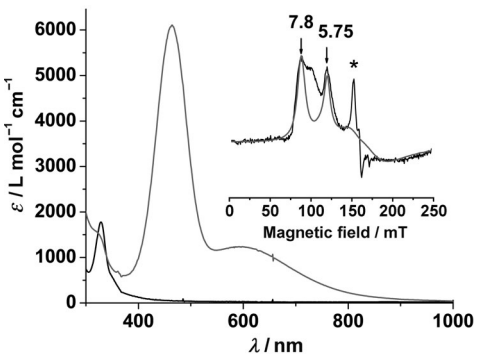

Figure 1. UV/Vis spectrum of **1** (black trace, 0.2 mM in 4:1 THF/DMF (v/v) at −90 °C) that reacted with KO_2 to yield **2** (gray trace). Molar absorptivity values were calculated using a combination of UV/Vis and Mössbauer experiments. Inset: X-band EPR spectrum of **2** in 4:1 THF/DMF. $T = 20$ K; microwave power, 2 mW, microwave frequency, 9.645 GHz, modulation amplitude, 10 G, modulation frequency, 100 Hz. Gray line is a theoretical spectrum for an $S = 5/2$ species with $E/D = 0.08$, and E/D distribution $\sigma(E/D) = 0.03$ (see text). The sharp feature marked with * arises from minor contaminant (ca. 0.5% of Fe). The high-field region is not shown as it is dominated by the intense absorption of free KO_2.

medium and a shift of the equilibrium back to **1** (Scheme 1).[6] Similar chemistry has been reported for a crown-ether-functionalized porphyrin ligand that facilitates the reversible formation of a heme–Fe^{III}(OO) complex from the heme–Fe^{II} precursor and KO_2.[7]

The highly chromophoric nature of **2** suggests that the iron center has been oxidized to Fe^{III}, concomitant with the reduction of the superoxide ligand to the peroxide level. However the electronic absorption spectrum of **2** is quite distinct from those reported for related non-heme RS-Fe^{III}-(OOX) (X = H or alkyl) complexes (Table 1). While all complexes exhibit broad absorption features in the 500–800 nm region typically associated with peroxo-to-Fe^{III} charge-transfer transitions, **2** has an additional feature at 460 nm ($\varepsilon = 6100\ L\,mol^{-1}\,cm^{-1}$) that is sharper and more intense (Figure 1). For comparison, treatment of [Fe^{II}(TMC)-(OTf)]$^+$ with KO_2 afforded a product with a broad band at 850 nm (Supporting Information, Figure S2), which is nearly identical to that observed for [Fe^{III}(TMC)(η^2-OO)]$^+$ in CH_3CN at −40 °C.[8] It would thus appear that the more basic axial ligand of **2** is required to elicit its novel absorption features. We therefore postulate that **2** represents a thus far unprecedented example of an RS-Fe^{III}(η^1-OO^-) complex.

EPR spectra of **2** revealed broad features belonging to an $S = 5/2$ species (Figure 1, inset). The spectra indicate that the rhombicity parameter, E/D, is distributed around a mean value of $E/D \approx 0.08$. The gray curve is an illustrative simulation for the major contributing species: the feature at $g = 7.9$ belongs to the $M_S = \pm 1/2$ ground doublet and the resonance $g = 5.75$ results from the $M_S = \pm 3/2$ excited state. The feature marked with the star is a minor rhombic contaminant (ca. 0.5% of total Fe; see the Supporting Information, Figure S5, for more details).[8b] The $S = 5/2$ species could arise from a ferromagnetically coupled ($S_{Fe^{II}} = 2/S_{superoxide} = 1/2$) center or from a high-spin Fe^{III} peroxide complex. The ^{57}Fe magnetic hyperfine interactions as well as the isomer shift of **2** obtained from Mössbauer spectra (Figure 2) establish that the iron center is in the high-spin ferric state.

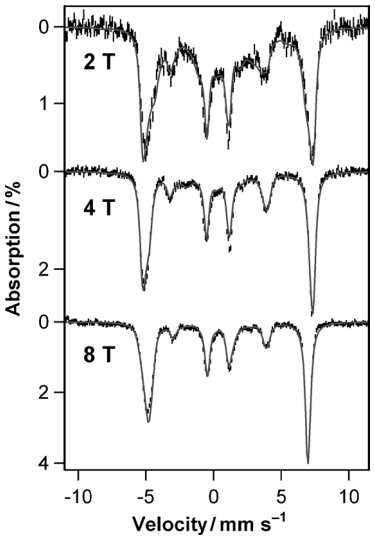

Figure 2. 4.2 K Mössbauer spectra of **2** recorded in parallel applied magnetic fields indicated in the figure. The gray curves are spectral simulations using the $S = 5/2$ spin-Hamiltonian of Equation (1) with $D = 2.5\ cm^{-1}$, $E/D = 0.08$, $g_{x,y,z} = 2.0$, $\delta = 0.71(3)\ mm\,s^{-1}$, $\Delta E_Q = -1.9(1)\ mm\,s^{-1}$, $\eta = -0.20$, $A_x/g_n\beta_n = A_y/g_n\beta_n = -17.5(4)$ T, $A_z/g_n\beta_n = -21.0(5)$ T.

We have simulated the 4.2 K Mössbauer spectra of **2** using the $S = 5/2$ spin Hamiltonian (parameters listed in the caption of Figure 2):

$$\mathscr{H} = D(S_z^2 - 35/4) + E(S_x^2 - S_y^2) + \beta \mathbf{S}\,\mathbf{g}\,\mathbf{B} + \mathbf{S}\,\mathbf{A}\,\mathbf{I} - g_n\beta_n\,\mathbf{B}\,\mathbf{I} + \mathscr{H}_Q \quad (1)$$

where D and E are the axial and rhombic zero-field splitting parameters, **A** is the ^{57}Fe magnetic hyperfine tensor, and $\mathscr{H}_Q$ describes the nuclear quadrupole interactions. $\Delta E_Q = (eQV_{zz}/12)(1+\eta^2/3)^{1/2}$ is the quadrupole splitting, while $\eta = (V_{xx} - V_{yy})/V_{zz}$ is the asymmetry parameter of the electric field gradient tensor. The shape of the Mössbauer spectrum recorded in an applied field, $B = 50$ mT (Supporting Information, Figure S6), just like the EPR spectrum, indicates that E/D is distributed; we were not able describe the E/D distribution by a symmetric function such as a Gaussian, and therefore we have focused the Mössbauer analysis on the high field spectra ($B \geq 2$ T), which are essentially independent of E/D. The 8.0 T spectrum reveals that **2** represents at least 95% of total Fe. Importantly, **2** has a negative quadrupole splitting, $\Delta E_Q = -1.9\ mm\,s^{-1}$, the largest value yet observed for a high-spin [Fe^{III}(TMC)] complex.[8b,11] The ^{57}Fe A tensor of **2** is characteristic of high-spin Fe^{III}. Its isotropic component, $A_{iso}/g_n\beta_n = -18.7$ T ($A_{iso} = (A_x + A_y + A_z)/3$), is comparable to the −20.0 T value reported for the high-spin Fe^{III}(TMC)(η^1-OOH) complex,[8b] and the smaller value observed for **2** can be attributed to the presence of the more covalent thiolate ligand. Interestingly,

the D and (dominant) E/D values of **2** are quite similar to those observed for $[Fe^{III}(TMC)(\eta^1\text{-}OOH)]^{2+}$ ($D = +2.5\ cm^{-1}$, $E/D = 0.097$).[8b] However the isomer shift of **2**, $\delta = 0.71(3)\ mm\,s^{-1}$, is distinctly larger than the $\delta = 0.51\ mm\,s^{-1}$ observed for $[Fe^{III}(TMC)(\eta^1\text{-}OOH)]^{2+}$.[8b]

The Mössbauer parameters of **2** reveal a high-spin ferric center with unique properties. It has the largest isomer shift for any Fe^{III} peroxide complex reported thus far,[8b,12] a large and negative ΔE_Q (with the largest component of the field gradient along z), and an ^{57}Fe A-tensor that is rather anisotropic for a high-spin Fe^{III} center.[13] These three properties have a common origin, as may be inferred from the following considerations. For a high-spin Fe^{III} center, the five d orbitals are occupied by α electrons. To explain the large and negative ΔE_Q, we postulate transfer of β electron density from the two filled peroxo π^* orbitals to the empty $\beta d_{xz}(Fe)$ and $\beta d_{yz}(Fe)$ orbitals. If only one orbital were involved (d_{xz} or d_{yz}), a positive ΔE_Q would result, with the largest component of the quadrupole tensor in the xy plane, in contrast to what is observed. However, if $\beta d_{xz}(Fe)$ and $\beta d_{yz}(Fe)$ were equally populated, a negative ΔE_Q with the major component along z would result, as observed.[14] As the spin-dipolar contribution to ^{57}Fe A tensor is proportional to the valence part of the quadrupole tensor, we expect the donation to increase the magnitude of A_z and to decrease the magnitude of $A_{x,y}$. Indeed, we observe that $|A_{x,y}| < |A_z|$. Finally, electron donation by the peroxo ligand into βd_{xz} and βd_{yz} orbitals enhances the d electron density at the iron, thereby imbuing the iron center with some ferrous character and resulting in an increase in its isomer shift as observed.

X-ray absorption spectroscopy (XAS) provided insight into the structural and electronic properties of **2**. The XAS edge energy of 7123.1 eV observed for **2** falls at the low energy end of the range reported for $Fe^{III}(OO)$ complexes (ca. 7123 to 7125 eV), consistent with an Fe^{III} center ligated by highly basic thiolate and peroxide donors (Supporting Information, Figure S8). There is a small pre-edge peak arising from a $1s \rightarrow 3d$ transition at 7113.6 eV with a peak area of 11.0 units (Supporting Information, Table S1), suggesting the presence of a fairly distorted six-coordinate Fe^{III} center.[15]

Analysis of EXAFS data for **2** yielded a principal shell of four N/O scatterers at 2.17 Å, which are attributed to the equatorial nitrogen donors of the TMCS ligand. This distance resembles that for $[Fe^{III}(TMC)(\eta^1\text{-}OOH)]^{2+}$ (2.15–2.16 Å) more closely than for its conjugate base $[Fe^{III}(TMC)(\eta^2\text{-}OO)]^{+}$ (2.20–2.23 Å).[8b,c] The inclusion of an S scatterer at 2.41 Å significantly improved the quality of the fit, indicating coordination of the thiolate moiety to the iron center. However the Fe–S distance found for **2** is rather long, relative to those observed for other synthetic RS-Fe^{III}(OOX) model complexes (ca. 2.30 Å), but comparable to values associated with biological RS-Fe^{III}(OOX) intermediates (Table 1). For the peroxo ligand, we considered two possible binding modes, η^2-side-on and η^1-end-on. Attempts to model **2** using an η^2-side-on peroxo moiety yielded unreasonably large σ^2 values (>15; Supporting Information, Table S2). In contrast, the inclusion of a single O/N scatterer at 1.89 Å significantly improved the quality of the fit (Supporting Information, Figure S9, Table S2). Taken together, the EXAFS fits favor a six-coordinate structure, with a pentadentate TMCS and an η^1-end-on peroxo moiety *trans* to the thiolate ligand.[16]

As the RS-$Fe^{III}(\eta^1\text{-}OO^-)$ complex would be expected to be prone to protonation, the reactivity of **2** towards weak acids was probed. The addition of 100 equiv 2,2,2-trifluoroethanol (TFE, $pK_a = 12.5$) to a solution of **2** resulted in the rapid (10 s) disappearance of the features assigned to **2** and the formation of new features ($\lambda_{max} = 550, 720$ nm) assigned to a new species **3** (Supporting Information, Figure S3). Under the same conditions, addition of 100 equiv of stronger acids such as ammonium acetate ($pK_a = 9.2$) or pyridinium triflate ($pK_a = 5.2$) also yielded intermediate **3** on the same time scale. In contrast, the reaction between **2** and 100 equiv MeOH ($pK_a = 15.2$) did not yield **3** but instead afforded **1**, presumably due to accelerated decay of KO_2 by disproportionation (Supporting Information, Figure S7).

The behavior of **1** with KO_2 is notably different from the RS-Fe^{II} complexes studied by Kovacs, for which no reaction with KO_2 was observed until the addition of MeOH, leading to the generation of RS-$Fe^{III}(\eta^1\text{-}OOH)$ intermediates.[4a,c] This was true even for the complex of the *N*-(3-*m*ercaptopropyl)-cyclam ligand,[4c] which is closely related to TMCS. In contrast, superoxide reduction readily occurred in the reaction between **1** and KO_2 in an aprotic solvent, to generate **2**, which could be easily protonated to yield a postulated RS-$Fe^{III}(\eta^1\text{-}OOH)$ intermediate (**3**) (Supporting Information, Scheme S1).

Reactivity studies provided further insights into the properties of the peroxide ligand in **2**. Complex **2** did not react at −90 °C with substrates that contain weak C–H bonds, such as dihydroanthracene, thus demonstrating that the bound peroxo moiety did not possess any electrophilic character. Its nucleophilic nature, however, was demonstrated in its reactivity towards electrophilic substrates. Menadione (2-methyl-1,4-naphthoquinone) is a substrate often used for this purpose, affording menadione epoxide (2,3-epoxy-2-methyl-1,4-naphthoquinone) in high yield (Supporting Information, Scheme S2).[17] For example, Valentine showed that $[Fe^{III}(F_{20}TPP)(\eta^2\text{-}OO)]^{-}$ ($F_{20}TPP$ = *meso*-tetrakis(pentafluorophenyl)porphinato) did not react with menadione in CH_3CN at 25 °C but afforded a 70 % yield of the epoxide product by change of solvent to dimethyl sulfoxide (DMSO).[17a,c] The latter reactivity was proposed to result from the binding of DMSO to the Fe^{III} center, converting the η^2-side-on peroxo moiety to its η^1-end-on isomer. When **2** was treated with menadione at −90 °C in 4:1 THF/DMF, menadione epoxide was obtained in 100 (±20) % yield within 60 s, supporting the assignment of **2** as an η^1-end-on peroxide complex.

Aldehyde substrates are also useful probes of metal peroxide nucleophilicity.[18] At −90 °C **2** reacted with 20 equiv of 2-phenylpropionaldehyde (PPA) within 5 s, yielding acetophenone and formate according to GC-MS. Accurate kinetic analysis, and thus determination of second order rate constants (k_2), at such rapid rates was not possible; however **2** was clearly a very active reactant for nucleophilic oxidation reactions. UV/Vis analysis of the reaction between **2** and PPA (Supporting Information, Figure S4) showed isosbestic behavior and a clean conversion to a new Fe^{III} product that displayed features typical of an RS-Fe^{III} complex

($\lambda_{max} = 480$ nm).[19] In stark contrast, we found that [Fe^{III}-(TMC)(η^2-OO)]$^+$ was not reactive towards PPA at −90 °C in 4:1 THF/DMF, in agreement with Nam's earlier report that side-on [Fe^{III}(TMC)(η^2-OO)]$^+$ was not reactive towards PPA at −40 °C.[8c] On the other hand, the end-on hydroperoxide analogue [Fe^{III}(TMC)(η^1-OOH)]$^{2+}$ reacted with PPA over the course of 800 s at −40 °C.[8c] Based on the accumulated observations on the reactivity of all the above Fe^{III}(L)(OO) complexes, it is clear that **2** contains a very reactive nucleophilic peroxide ligand, which reacts rapidly, even at −90 °C. These results further support our assignment of **2** as an RS-Fe^{III}(η^1-OO^-) complex.

In summary, the reaction between an RS-Fe^{II} complex **1** and KO_2 at −90 °C in aprotic solvent generates a reversible adduct **2** that is best described as an RS-Fe^{III}(η^1-OO^-) complex on the basis of its spectroscopic properties. We postulate that **2** represents the first synthetic model of the initial SOR-superoxide adduct prior to its protonation in the SOR catalytic cycle. Two recent DFT studies favor an RS-Fe^{II}($OO^{\bullet}$) description for this adduct using simplified active sites that did not include second sphere residues.[3d,20] However our results provide experimental evidence that the isomeric RS-Fe^{III}(η^1-OO^-) complex can be generated and stabilized in an aprotic medium and in fact exhibits an absorption band at 610 nm like that found for the SOR intermediate.[3] For **2**, the dianionic peroxo ligand may be stabilized in part by the potassium ion introduced through the use of KO_2. Related porphyrin–Fe^{III}(OO^-) complexes have been reported, but they do not have an axial thiolate ligand.[7,21] **2**, therefore, is a unique example of a thiolato iron(III) peroxy dianion model compound that mimics the structure and function of the postulated RS-Fe^{III}(η^1-OO^-) intermediates in SOR and the P450 family. We have also shown that the peroxide ligand on **2** is highly nucleophilic in nature and is readily protonated by weak acids, consistent with a possible role for this species in the SOR cycle. Furthermore, **2** reacts rapidly with carbonyl compounds, even at −90 °C, making it relevant to the nucleophilic chemistry postulated for corresponding RS-Fe^{III}(η^1-OO^-) intermediates in the catalytic cycles of heme–thiolate enzymes, such as aromatase and NO synthase.[18,22]

Received: May 9, 2012
Revised: June 19, 2012
Published online: August 7, 2012

Keywords: bioinorganic chemistry · iron · peroxo intermediates · reactive intermediates · thiolate complexes

[1] a) V. Nivière, F. Bonnot, D. Bourgeois in *Handbook of Metalloproteins*, *Vols. 4 & 5* (Ed.: A. Messerschmidt), Wiley, Chichester, **2011**, pp. 246–258; b) A. S. Pereira, P. Tavares, F. Folgosa, R. M. Almeida, I. Moura, J. J. G. Moura, *Eur. J. Inorg. Chem.* **2007**, 2569–2581; c) D. M. Kurtz, Jr., *Acc. Chem. Res.* **2004**, *37*, 902–908.

[2] a) C. Mathé, C. O. Weill, T. A. Mattioli, C. Berthomieu, C. Houée-Levin, E. Tremey, V. Nivière, *J. Biol. Chem.* **2007**, *282*, 22207–22216; b) J. A. Kovacs, L. M. Brines, *Acc. Chem. Res.* **2007**, *40*, 501–509.

[3] a) M. Lombard, C. Houée-Levin, D. Touati, M. Fontecave, V. Nivière, *Biochemistry* **2001**, *40*, 5032–5040; b) C. Mathé, T. A. Mattioli, O. Horner, M. Lombard, J.-M. Latour, M. Fontecave, V. Nivière, *J. Am. Chem. Soc.* **2002**, *124*, 4966–4967; c) V. Nivière, M. Asso, C. O. Weill, M. Lombard, B. Guigliarelli, V. Favaudon, C. Houée-Levin, *Biochemistry* **2004**, *43*, 808–818; d) F. Bonnot, T. Molle, S. Ménage, Y. Moreau, S. Duval, V. Favaudon, C. Houée-Levin, V. Nivière, *J. Am. Chem. Soc.* **2012**, *134*, 5120–5130; e) E. D. Coulter, J. P. Emerson, D. M. Kurtz, Jr., D. E. Cabelli, *J. Am. Chem. Soc.* **2000**, *122*, 11555–11556; f) J. P. Emerson, E. D. Coulter, D. E. Cabelli, R. S. Phillips, D. M. Kurtz, Jr., *Biochemistry* **2002**, *41*, 4348–4357.

[4] a) J. Shearer, R. C. Scarrow, J. A. Kovacs, *J. Am. Chem. Soc.* **2002**, *124*, 11709–11717; b) D. Krishnamurthy, G. D. Kasper, F. Namuswe, W. D. Kerber, A. A. N. Sarjeant, P. Moenne-Loccoz, D. P. Goldberg, *J. Am. Chem. Soc.* **2006**, *128*, 14222–14223; c) T. Kitagawa, A. Dey, P. Lugo-Mas, J. B. Benedict, W. Kaminsky, E. Solomon, J. A. Kovacs, *J. Am. Chem. Soc.* **2006**, *128*, 14448–14449; d) F. Namuswe, G. D. Kasper, A. A. N. Sarjeant, T. Hayashi, C. M. Krest, M. T. Green, P. Moenne-Loccoz, D. P. Goldberg, *J. Am. Chem. Soc.* **2008**, *130*, 14189–14200; e) Y. Jiang, J. Telser, D. P. Goldberg, *Chem. Commun.* **2009**, 6828–6830; f) F. Namuswe, T. Hayashi, Y. Jiang, G. D. Kasper, A. A. N. Sarjeant, P. Moenne-Loccoz, D. P. Goldberg, *J. Am. Chem. Soc.* **2010**, *132*, 157–167; g) J. Stasser, F. Namuswe, G. D. Kasper, Y. Jiang, C. M. Krest, M. T. Green, J. Penner-Hahn, D. P. Goldberg, *Inorg. Chem.* **2010**, *49*, 9178–9190; h) E. Nam, P. E. Alokolaro, R. D. Swartz, M. C. Gleaves, J. Pikul, J. A. Kovacs, *Inorg. Chem.* **2011**, *50*, 1592–1602.

[5] A. T. Fiedler, H. L. Halfen, J. A. Halfen, T. C. Brunold, *J. Am. Chem. Soc.* **2005**, *127*, 1675–1689.

[6] As peroxide is a byproduct of superoxide disproportionation, control experiments between **1** and H_2O_2 or Na_2O_2 were carried out in THF/DMF at −90 °C. In neither case was a reaction observed over the course of 1 h.

[7] a) K. Dürr, B. P. Macpherson, R. Warratz, F. Hampel, F. Tuczek, M. Helmreich, N. Jux, I. Ivanovic-Burmazovic, *J. Am. Chem. Soc.* **2007**, *129*, 4217–4228; b) K. Dürr, N. Jux, A. Zahl, R. van Eldik, I. Ivanovic-Burmazovic, *Inorg. Chem.* **2010**, *49*, 11254–11260; c) K. Duerr, J. Olah, R. Davydov, M. Kleimann, J. Li, N. Lang, R. Puchta, E. Hubner, T. Drewello, J. N. Harvey, N. Jux, I. Ivanovic-Burmazovic, *Dalton Trans.* **2010**, *39*, 2049–2056.

[8] a) J. Annaraj, Y. Suh, M. S. Seo, S. O. Kim, W. Nam, *Chem. Commun.* **2005**, 4529–4531; b) F. Li, K. K. Meier, M. A. Cranswick, M. Chakrabarti, K. M. Van Heuvelen, E. Münck, L. Que, Jr., *J. Am. Chem. Soc.* **2011**, *133*, 7256–7259; c) J. Cho, S. Jeon, S. A. Wilson, L. V. Liu, E. A. Kang, J. J. Braymer, M. H. Lim, B. Hedman, K. O. Hodgson, J. S. Valentine, E. I. Solomon, W. Nam, *Nature* **2011**, *478*, 502–505.

[9] a) A. P. Yeh, Y. Hu, F. E. Jenney, M. W. W. Adams, D. C. Rees, *Biochemistry* **2000**, *39*, 2499–2508; b) G. Katona, P. Carpentier, V. Nivière, P. Amara, V. Adam, J. Ohana, N. Tsanov, D. Bourgeois, *Science* **2007**, *316*, 449–453.

[10] K. Kühnel, E. Derat, J. Terner, S. Shaik, I. Schlichting, *Proc. Natl. Acad. Sci. USA* **2007**, *104*, 99–104.

[11] J. F. Berry, E. Bill, E. Bothe, F. Neese, K. Wieghardt, *J. Am. Chem. Soc.* **2006**, *128*, 13515–13528.

[12] M. Costas, M. P. Mehn, M. P. Jensen, L. Que, Jr., *Chem. Rev.* **2004**, *104*, 939–986.

[13] G. Lang, *Q. Rev. Biophys.* **1970**, *3*, 1–60.

[14] The valence contribution to the principal components of the quadrupole tensor ($Q'_{xx,yy,zz}$, in atomic units) is proportional to (−2/7, +4/7, −2/7) and (+4/7, −2/7, −2/7) for an electron in d_{xz} and d_{yz}, respectively. Adding these contributions yields (2/7, 2/7, −4/7). See: P. Gütlich, R. Link, A. Trautwein, *Mössbauer*

Spectroscopy and Transition Metal Chemistry, Springer, Berlin, **1978**.

[15] S. DeBeer George, T. Petrenko, F. Neese, *J. Phys. Chem. A* **2008**, *112*, 12936 – 12943.

[16] Because of the importance of vibrational information, we made a number of attempts to obtain such data to probe the peroxide binding mode in **2**, but these experiments were all unsuccessful. These experiments are described in the Supporting Information.

[17] a) M. Selke, M. F. Sisemore, J. S. Valentine, *J. Am. Chem. Soc.* **1996**, *118*, 2008 – 2012; b) M. F. Sisemore, J. N. Burstyn, J. S. Valentine, *Angew. Chem.* **1996**, *108*, 195 – 196; *Angew. Chem. Int. Ed. Engl.* **1996**, *35*, 206 – 208; c) M. Selke, J. S. Valentine, *J. Am. Chem. Soc.* **1998**, *120*, 2652 – 2653.

[18] D. L. Wertz, J. S. Valentine, *Struct. Bonding (Berlin)* **2000**, *97*, 38 – 60.

[19] a) P. Kennepohl, F. Neese, D. Schweitzer, H. L. Jackson, J. A. Kovacs, E. I. Solomon, *Inorg. Chem.* **2005**, *44*, 1826 – 1836; b) M. R. Bukowski, K. D. Koehntop, A. Stubna, E. L. Bominaar, J. A. Halfen, E. Münck, W. Nam, L. Que, Jr., *Science* **2005**, *310*, 1000 – 1002.

[20] A. Dey, F. E. Jenney, M. W. W. Adams, M. K. Johnson, K. O. Hodgson, B. Hedman, E. I. Solomon, *J. Am. Chem. Soc.* **2007**, *129*, 12418 – 12431.

[21] J.-G. Liu, Y. Shimizu, T. Ohta, Y. Naruta, *J. Am. Chem. Soc.* **2010**, *132*, 3672 – 3673.

[22] a) M. R. C. M. Akhtar, D. L. Corina, J. N. Wright, *Biochem. J.* **1982**, *201*, 569 – 580; b) K. R. Korzekwa, W. F. Trager, S. J. Smith, Y. Osawa, J. R. Gillette, *Biochemistry* **1991**, *30*, 6155 – 6162; c) R. A. Pufahl, J. S. Wishnok, M. A. Marletta, *Biochemistry* **1995**, *34*, 1930 – 1941; d) J. J. Woodward, M. M. Chang, N. I. Martin, M. A. Marletta, *J. Am. Chem. Soc.* **2009**, *131*, 297 – 305.

